J. Fluid Mech. (1997), *vol.* 336, *pp.* 203–220

Intense vortex motion in a stratified fluid on the beta-plane: an analytical theory and its validation

By GEORGI G. SUTYRIN[1] AND YVES G. MOREL[2]

[1]Russian Academy of Sciences, P. P. Shirshov Institute of Oceanology, 23 Krasikova Street, Moscow, 117256 Russia

[2]EPSHOM/CMO, BP 426, 29275, Brest CEDEX, France

(Received 27 March 1996 and in revised form 11 November 1996)

This paper deals with the self-induced translation of intense vortices on the β-plane in the framework of the multi-layer quasi-geostrophic approximation. An analytical theory is presented and compared to numerical experiments. To predict the vortex trajectories, we consider initially monopolar vortices, with a core of piecewise-constant potential vorticity, and calculate the evolution of the dipolar circulation which advects the vortex core. This multi-layer model yields analytical solutions for a period while the Rossby wave radiation is small.

The development of the dipolar circulation and corresponding vortex translation are described as the results of three effects. The first and second are similar to what was found in earlier studies with a one-layer model: advection of the planetary vorticity by the symmetric vortex circulation, and horizonal deformations of the vortex core. In addition, when stratification is taken into account, the vertical tilting of the vortex core also plays a role. This third effect is here represented by the relative displacement of potential vorticity contours in different layers.

Examples are given for one-, two- and three-layer models and compared with numerical simulations. It is found that the analytical predictions are good for several Rossby wave periods.

1. Introduction

In geophysical fluid dynamics, the effect of vortices on large-scale flows depends on their strength and lifetime. For instance, weak eddies from the mesoscale turbulence have a lifetime of several days to several weeks and their effect on large-scale flows is mainly to mix tracers along isopycnic surfaces. On the other hand, intense coherent vortices are long-lived patterns and can have different transport properties. Indeed, atmospheric hurricanes, oceanic rings and lenses sometimes carry trapped fluid over thousands of kilometres (Khain & Sutyrin 1983; Kamenkovich, Koshlyakov & Monin 1986) apparently along preferred paths or directions, which therefore represents an anisotropic transport. For instance, the Mediterranean salt tongue extending south-west of Gibraltar is commonly attributed to Mediterranean water vortices (McWilliams 1985). Various mechanisms responsible for the generation and propagation of these coherent structures have been studied during the last few decades, but much work still needs to be done to understand their evolution in a stratified fluid.

Observations show that anticyclones move preferentially south-westward and cyclones north-westward. This is considered to result mainly from the variation of the Coriolis parameter with latitude (the beta-effect). For one-layer models, the physical mechanisms responsible for the self-induced vortex propagation have been elucidated. As shown by Sutyrin (1987, 1988, 1989*a*) for a finite radius of deformation as well as by Smith & Ulrich (1990) and Peng & Williams (1990) for an infinite radius of deformation (where the radius of deformation is defined by the ratio of gravity wave speed to the Coriolis parameter), the vortex is advected by a dipolar circulation generated when a monopolar vortex evolves in an ambient fluid with a background gradient of potential vorticity. This dipolar circulation has also been detected in numerical simulations and called 'beta-gyre' (McWilliams & Flierl 1979; Fiorino & Elsberry 1989; Smith, Ulrich & Dietachmayer 1990).

An explicit description of the beta-gyre evolution has been developed by Sutyrin & Flierl (1994, referred to herein as SF94), for a piecewise-constant potential vorticity distribution of an initially axisymmetric vortex, in a one-layer quasi-geostrophic model with an arbitrary radius of deformation (see also Sutyrin *et al.* 1994). In the particular case of infinite radius of deformation, Reznik & Dewar (1994) found an analytical solution for an arbitrary initial vortex. These studies have shown that the dipolar circulation and corresponding vortex translational velocity were induced by the generation of a potential vorticity anomaly when planetary vorticity is advected and rotated differentially by the symmetric vortex circulation, and by the horizontal deformations of the vortex core. However, numerical simulations have indicated that baroclinic mechanisms could also strongly influence the vortex motion, depending on the vortex structure and background stratification (McWilliams & Flierl 1979; Chassignet & Cushman-Roisin 1991; Shapiro 1992; Flatau, Schubert & Stevens 1994; Morel & McWilliams 1996).

In this paper we describe an analytical model that yields an explicit solution for the propagation speed of a strong vortex whose potential vorticity structure is piecewise constant, generalizing the SF94 approach to a multi-layer stratified fluid. By comparing the analytic solution to numerical experiments, we found that the deviation of the vortex position from the predicted one does not exceed 20% of the vortex radius for several Rossby wave periods, $T_R = 1/\beta R$ (where β is the gradient of planetary vorticity and R the lengthscale of the vortex). The solution provides useful insights into basic mechanisms governing the baroclinic vortex motion on the beta-plane. The relationships between the background stratification, the vortex structure and its dynamics will be studied in detail in a forthcoming paper.

In §2, we present the mathematical framework, the quasi-geostrophic multilayer equations and the numerical algorithm. Next, in §3, we derive analytical expressions for the dipolar component of the flow and the vortex trajectory. In §4, we then test this analytical model and compare the theoretical results with numerical solutions. The last section contains a summary and a discussion of the results.

2. Quasi-geostrophic multi-layer model

2.1. *Equations*

We will restrict our attention hereafter to intense vortices for which the Coriolis force dominates the relative acceleration (small Rossby number, $R_o = U/fL \ll 1$) and with moderate isopycnal deviations. The motions are thus described by a quasigeostrophic model on the β-plane whose inviscid equations rely on the conservation of potential

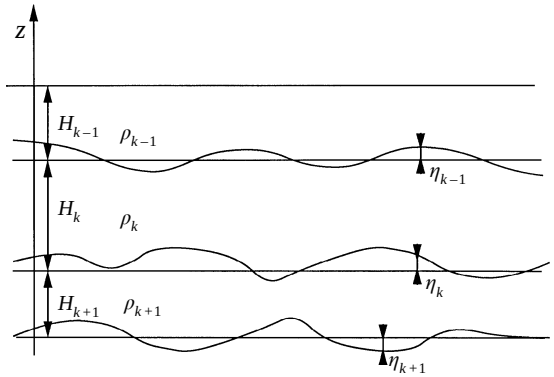

FIGURE 1. Description of the inner part of the model.

vorticity. For a multi-layer stratified fluid, the equations are (see Pedlosky 1987, chap. 6.16)

$$\frac{\partial PV_k}{\partial T} + \frac{\partial(\Psi_k, PV_k)}{\partial(X,Y)} + \beta\frac{\partial \Psi_k}{\partial X} = 0, \tag{1a}$$

$$PV_k = \nabla^2\Psi_k + f_0\frac{\xi_{k-1} - \xi_k}{H_k}, \tag{1b}$$

$$\xi_k = \frac{\rho_1 f_0}{g}\frac{\Psi_{k+1} - \Psi_k}{\rho_{k+1} - \rho_k}, \tag{1c}$$

where Ψ_k and PV_k are the streamfunction and potential vorticity anomaly in the kth layer, T is the time, X and Y are eastward and polarward coordinates, respectively, f_0 is the Coriolis frequency, H_k is the unperturbed depth of the kth layer, and ξ_k is the displacement of the interface between layers having densities ρ_k and ρ_{k+1}, so that $\xi_{k-1} - \xi_k$ represents the vortex stretching (figure 1). Notice that $(1b, c)$ are only valid for internal layers. For the surface and bottom layers, boundary conditions are necessary. We will make the rigid-lid approximation for the upper layer and consider either the flat bottom case or an infinitely deep and passive lower layer. The potential vorticity in the first layer is then

$$PV_1 = \nabla^2\Psi_1 + \frac{\rho_1 f_0^2}{gH_1}\frac{\Psi_2 - \Psi_1}{\rho_2 - \rho_1} \tag{1d}$$

and the potential vorticity in the last active layer is given by

$$PV_N = \nabla^2\Psi_N + \frac{\rho_1 f_0^2}{gH_N}\frac{\Psi_{N-1} - \Psi_N}{\rho_N - \rho_{N-1}} - \Upsilon\frac{\rho_1 f_0^2}{gH_N}\frac{\Psi_N}{\rho_{N+1} - \rho_N}, \tag{1e}$$

where N is the number of active layers, and $\Upsilon = 0$ for the flat bottom case and $\Upsilon = 1$ if we consider an infinitely deep and passive layer with density ρ_{N+1} below the Nth layer.

The conservation of total potential vorticity ($\Gamma_k = \beta Y + PV_k$) by fluid particles in each layer is ensured by $(1a)$. When β is not zero, the fluid rotation in the vortex produces the potential vorticity anomalies which induce the corresponding secondary flows (the beta-gyres) responsible for the self-propagation of the vortex. The problem is to calculate both the beta-gyres and the vortex-centre trajectory $(X_0(T), Y_0(T))$ (to be defined precisely later), given the initial vortex structure $\Psi_k(X, Y, 0)$.

2.2. *Numerical algorithm*

Equations (1*a–c*) will be solved numerically with a pseudo-spectral code in the horizontal (biperiodic domain with a 128×128 horizontal grid in each layer, Orszag 1971).

A biharmonic viscosity is used to avoid computational instability. Viscosity does not affect the evolution of the vortex for the period of time considered in this paper. The time step is $\Delta T = 0.025$ non-dimensional time units (see below) and the model is typically run for 100 units. The periodic continuation of the Rossby wave wake generated by the displacement of the vortex does not interfere with the vortex core during this short period.

3. Analytical theory

3.1. *Change of coordinates*

In this study, we will concentrate on vortices with a strong axisymmetric part. We take advantage of this by using cylindric coordinates with the origin at the vortex centre.

Let us introduce a characteristic horizontal scale of the vortex $\hat{R}$, a vertical scale $\hat{H}$, a vortex rotation rate $\hat{\Omega}$ and the polar coordinates (r, θ) defined as $r\cos\theta = (X - X_0)/\hat{R}$, $r\sin\theta = (Y - Y_0)/\hat{R}$. Equation (1*a–c*) can be rewritten in non-dimensional form and with these new coordinates

$$\frac{\partial}{\partial t}\omega_k + J(\psi_k^*, \omega_k) + \epsilon J(\psi_k, r\sin\theta) = 0, \tag{2a}$$

$$\nabla^2\psi_k + \frac{s_{k-1}}{h_k}(\psi_{k-1} - \psi_k) + \frac{s_k}{h_k}(\psi_{k+1} - \psi_k) = \omega_k, \tag{2b}$$

where $t = \hat{\Omega}T$, $\omega_k = PV_k/\hat{\Omega}$, $\psi_k = \Psi_k/\hat{\Omega}\hat{R}^2$; the parameters

$$s_k = \frac{\rho_1 f_0^2 \hat{R}^2}{(\rho_{k+1} - \rho_k)g\hat{H}}, \qquad h_k = \frac{H_k}{\hat{H}}, \qquad \epsilon = \frac{\beta\hat{R}}{\hat{\Omega}} \tag{2c}$$

characterize the stretching effects, the non-dimensional layer depth and the β-effect, respectively;

$$\psi_k^* = \psi_k + \epsilon u r\sin\theta - \epsilon v r\cos\theta$$

where $(u, v) = (\dot{X}_0/\beta\hat{R}^2, \dot{Y}_0/\beta\hat{R}^2)$ is the translational velocity of the vortex centre; and $J(A, B) = (1/r)\,[\partial_r A\partial_\theta B - \partial_r B\partial_\theta A]$ is the Jacobian of A and B expressed in polar coordinates.

Equations (2*a,b*) are analytically intractable, but following SF94, an approximate analytical solution valid for a non-dimensional timescale smaller than $(\epsilon r_0)^{-1}$ (where r_0 is the non-dimensional radius of the vortex) can be found.

3.2. *Contour dynamical model*

Let us now assume that the potential vorticity structure of the vortex is initially axisymmetric and piecewise constant. We thus set in each layer

$$\psi_k = \Phi_k + \epsilon\phi_k\ , \quad \omega_k = Q_k + \epsilon q_k,$$

where ϕ_k and q_k represents the beta-gyres and Φ_k is the streamfunction associated with the piecewise-constant potential vorticity part of the vortex

$$Q_k = \sum_j \Delta_{k,j} \mathscr{H}(r_{k,j} + \epsilon\eta_{k,j} - r). \tag{3}$$

Here, $\mathscr{H}$ is the Heaviside function, $\Delta_{k,j} = Q_{k,j+1} - Q_{k,j}$ is the potential vorticity jump at the jth boundary $r = r_{k,j} + \epsilon\eta_{k,j}(\theta, t)$ between different potential vorticity regions in the kth layer, $r_{k,j}$ is the unperturbed (initial) radius of the boundary, and $\epsilon\eta_{k,j}$ represents the distortions of the vortex core.

As gradients of Q_k give delta functions, we get

$$\frac{\mathrm{D}}{\mathrm{D}t} Q_k = \sum_j \Delta_{k,j} \delta(r_{k,j} + \epsilon\eta_{k,j} - r) \left[\epsilon \frac{\mathrm{D}}{\mathrm{D}t} \eta_{k,j} - \frac{\mathrm{D}}{\mathrm{D}t} r \right]$$

Assuming that q_k is continuous and equating the coefficients for all the delta function terms to zero gives at each boundary

$$\frac{\partial}{\partial t}\eta + \frac{V_\theta}{r}\frac{\partial}{\partial \theta}\eta = V_r = -\frac{1}{r}\frac{\partial}{\partial \theta}\psi.$$

This then yields

$$\frac{\partial}{\partial t}\eta_{k,j} + \Omega_{k,j}\frac{\partial}{\partial \theta}\eta_{k,j} + \frac{1}{r_{k,j} + \epsilon\eta_{k,j}}\frac{\partial}{\partial \theta}\frac{1}{\epsilon}\Phi_{k,j} = -\frac{1}{r_{k,j} + \epsilon\eta_{k,j}}\frac{\partial}{\partial \theta}\phi^*_{k,j} \tag{4a}$$

with

$$\Omega_{k,j} = \frac{1}{r_{k,j} + \epsilon\eta_{k,j}}\frac{\partial}{\partial r}(\Phi_{k,j} + \epsilon\phi^*_{k,j}),$$

$$\phi^*_{k,j} = \phi_{k,j} + ur\sin\theta - vr\cos\theta,$$

and $\Phi_{k,j} = \Phi_k(r_{k,j} + \epsilon\eta_{k,j}, \theta, t)$. Taking (4$a$) into account, (2$a$) yields the forced Rossby wave equation that q_k and ϕ_k must satisfy:

$$\frac{\partial}{\partial t} q_k + \epsilon J(\phi^*_k, q_k) + \epsilon J(\phi_k, r\sin\theta) + J(\Phi_k, q_k) = -J(\Phi_k, r\sin\theta), \tag{4b}$$

$$q_k = \nabla^2\phi_k + \frac{s_{k-1}}{h_k}(\phi_{k-1} - \phi_k) + \frac{s_k}{h_k}(\phi_{k+1} - \phi_k), \tag{4c}$$

Notice that up to now, no approximations have been made. If there were no β-effect, the $r\sin\theta$ terms would disappear from (4b), and we could consistently set ϕ_k and q_k to zero. Then (3) and (4a) would form a standard contour-dynamical problem (cf. Polvani, Zabusky & Flierl 1989).

3.3. *Linearization*

If the vortex is strong enough, we can consider ϵ to be a small parameter and use a multi-timescale expansion. We then decompose the vortex flow into an axisymmetric part and asymmetric perturbations:

$$\Phi_k = \overline{\Phi}_k(r, t, \epsilon t) + \epsilon\Phi'_k(r, \theta, t, \epsilon t).$$

Averaging (4a) over θ shows that, at leading order and for a non-dimensional timescale which is smaller than $(\epsilon r_0)^{-1}$ (where r_0 is the non-dimensional lengthscale

characterizing the vortex), the radially symmetric part of the vortex $\overline{\Phi}_k$ keeps its initial structure and satisfies

$$\nabla^2\overline{\Phi}_k + \frac{s_{k-1}}{h_k}(\overline{\Phi}_{k-1} - \overline{\Phi}_k) + \frac{s_k}{h_k}(\overline{\Phi}_{k+1} - \overline{\Phi}_k) = \sum_j \Delta_{k,j}\mathscr{H}(r_{k,j} - r)$$

according to (3). Differentiating this, we find an equation for the azimuthal velocity $\overline{V} = \mathrm{d}\overline{\Phi}/\mathrm{d}r$:

$$\left(\nabla^2 - \frac{1}{r^2}\right)\overline{V}_k + \frac{s_{k-1}}{h_k}(\overline{V}_{k-1} - \overline{V}_k) + \frac{s_k}{h_k}(\overline{V}_{k+1} - \overline{V}_k) = -\sum_j \Delta_{k,j}\delta(r_{k,j} - r). \quad (5)$$

while Φ'_k then satisfies the equation

$$\nabla^2\Phi'_k + \frac{s_{k-1}}{h_k}(\Phi'_{k-1} - \Phi'_k) + \frac{s_k}{h_k}(\Phi'_{k+1} - \Phi'_k) = \frac{1}{\epsilon}\sum_j \Delta_{k,j}[\mathscr{H}(r_{k,j} + \epsilon\eta_{k,j} - r) - \mathscr{H}(r_{k,j} - r)]$$

which gives at leading order in the small-ϵ limit

$$\nabla^2\Phi'_k + \frac{s_{k-1}}{h_k}(\Phi'_{k-1} - \Phi'_k) + \frac{s_k}{h_k}(\Phi'_{k+1} - \Phi'_k) = \sum_{k,j} \Delta_{k,j}\eta_{k,j}\delta(r - r_{k,j}). \quad (6a)$$

Linearizing the dynamical equation (4*a*,*b*) yields

$$\frac{\partial}{\partial t}\eta_{k,j} + \overline{\Omega}_{k,j}\frac{\partial}{\partial\theta}\eta_{k,j} + \frac{1}{r_{k,j}}\frac{\partial}{\partial\theta}\Phi'_{k,j} = -\frac{1}{r_{k,j}}\frac{\partial}{\partial\theta}\phi_{k,j} - u\cos\theta - v\sin\theta, \quad (6b)$$

$$\frac{\partial}{\partial t}q_k + \overline{\Omega}_k\frac{\partial}{\partial\theta}q_k = -\overline{\Omega}_k r\cos\theta, \quad (6c)$$

with

$$\overline{\Omega}_k(r) \equiv \frac{\overline{V}_k}{r}$$

and

$$q_k = \nabla^2\phi_k + \frac{s_{k-1}}{h_k}(\phi_{k-1} - \phi_k) + \frac{s_k}{h_k}(\phi_{k+1} - \phi_k). \quad (6d)$$

Thus, the first part of the beta-gyres is generated directly by advection of planetary vorticity and is described by (6*c*). The second part of the beta-gyres is induced by distortions in the vortex core due to radial advection of contours relative to the vortex centre by the first part of the beta-gyres (equation (6*b*)).

3.4. *Solutions*

Assuming that $q_k = 0$ at $t = 0$, equation (6*c*) is easily integrated for each layer:

$$q_k = r\sin(\theta - \overline{\Omega}_k t) - r\sin\theta = \mathrm{Re}[\mathrm{i}r\,(\mathrm{e}^{\mathrm{i}\overline{\Omega}_k t} - 1)\mathrm{e}^{-\mathrm{i}\theta}]. \quad (6e)$$

For the timescales considered here, the dominant response is in the azimuthal mode number one and the residual motion has a dipolar structure. Thus, we set $\phi_k = \mathrm{Re}(\phi_k\mathrm{e}^{-\mathrm{i}\theta})$, $\Phi'_k = \mathrm{Re}(\Phi'_k\mathrm{e}^{-\mathrm{i}\theta})$, $\eta_{k,j} = \mathrm{Re}(\eta_{k,j}\mathrm{e}^{-\mathrm{i}\theta})$ (for the sake of simplicity, the same notation has been used for each real quantity and its associated imaginary radial part).

Equations (5) and (6*a–d*) can be solved using vertical modes. We find (see Appendix A)

$$\overline{\Omega}_k(r) \equiv \frac{\overline{V}_k}{r} = -\frac{1}{r}\sum_{n,l,j} P_k^{(n)}\alpha_l^{(n)}\Delta_{l,j}G_1^{(n)}(r|r_{l,j}), \quad (7a)$$

$$\Phi'_k(r,t) = \sum_{n,l,j} P_k^{(n)} \alpha_l^{(n)} \Delta_{l,j} \eta_{l,j} G_1^{(n)}(r|r_{l,j}), \tag{7b}$$

and

$$\phi_k = \mathrm{i} \sum_{n,l} P_k^{(n)} \alpha_l^{(n)} \; F_l^{(n)}, \tag{7c}$$

where

$$F_l^{(n)}(r,t) = \int r' \mathrm{d}r' G_1^{(n)}(r|r')(\mathrm{e}^{\mathrm{i}\overline{\Omega}_l(r')t} - 1) \tag{7d}$$

which can alternatively be expressed as

$$F_l^{(n)} = \frac{r}{\gamma_n^2} - I_1(\gamma_n r) \int_r^\infty K_1(\gamma_n r') \mathrm{e}^{\mathrm{i}\overline{\Omega}_l t} r'^2 \mathrm{d}r' - K_1(\gamma_n r) \int_0^r I_1(\gamma_n r') \mathrm{e}^{\mathrm{i}\overline{\Omega}_l t} r'^2 \mathrm{d}r'.$$

In these solutions, $\boldsymbol{P}^{(n)} = (P_1^{(n)}, ..., P_k^{(n)}, ..., P_N^{(n)})$ is the nth vertical eigenmode associated with the stretching operator (see Appendix A) and $-\gamma_n^2$ is its corresponding eigenvalue. The $N \times N$ matrix $\boldsymbol{\alpha}$ with coefficients $\alpha_l^{(n)}$ is the inverse of the matrix $\boldsymbol{P}$ whose columns are the vectors $\boldsymbol{P}^{(n)}$. $G_1^{(n)}$ is the Green function associated with the Helmholtz operator $((r\partial_r(r\partial_r) - 1)/r^2 - \gamma_n^2)$, and is expressed in terms of modified Bessel functions K_1 and I_1 (see Appendix A).

3.5. *Propagation speed*

Equations (6*b*) and (7*a–c*) yield

$$\frac{\partial}{\partial t}\eta_{k,j} - \mathrm{i} \sum_{l,i} A_{k,j;l,i} \eta_{l,i} = \mathrm{i} \frac{\phi_{k,j}}{r_{k,j}} - u - \mathrm{i}v, \tag{8a}$$

where

$$A_{k,j;l,i} = \overline{\Omega}(r_{k,j}) \delta_{kl} \delta_{ij} + \frac{1}{r_{k,j}} \sum_n P_k^{(n)} \alpha_l^{(n)} \Delta_{l,i} G_1^{(n)}(r_{k,j}|r_{l,i}) \tag{8b}$$

and

$$\phi_{k,j} = \mathrm{i} \sum_{n,l} P_k^{(n)} \alpha_l^{(n)} F_l^{(n)}(r_{k,j}, t)$$

according to (7*c*).

To solve (8*a*), we must choose a definition for the vortex centre. As discussed in SF94, the most appropriate choice is the centre of one contour. We then set $\eta_{k_0,j_0} = 0$ in (8*a*), where k_0, j_0 refers to the chosen contour (j_0th contour in the k_0th layer).

This then allows us to calculate the propagation speed

$$u + \mathrm{i}v = \mathrm{i} \sum_{l,i} A_{k_0,j_0;l,i} \; \eta_{l,i} + \mathrm{i} \frac{\phi_{k_0,j_0}}{r_{k_0,j_0}}, \tag{9a}$$

and replacing $u + \mathrm{i}v$ by the right-hand side of (9*a*) permits us to calculate the $\eta_{l,i}$ independently of the propagation speed for all the other contours which correspond to distortions of the vortex. We get

$$\frac{\partial}{\partial t}\eta_{k,j} - \mathrm{i} \sum_{l,i} B_{k,j;l,i} \eta_{l,i} = \mathrm{i} \frac{\phi_{k,j}}{r_{k,j}} - \mathrm{i} \frac{\phi_{k_0,j_0}}{r_{k_0,j_0}} \tag{9b}$$

with

$$B_{k,j;l,i} = A_{k,j;l,i} - A_{k_0,j_0;l,i}.$$

Equation (9*b*) is an ODE and is easily solved using normal modes; i.e. the free solutions to (9*b*) with time–dependence $e^{i\sigma t}$, which are eigenvectors of matrix $\boldsymbol{B}$:

$$\sum_{l,i} B_{k,j;l,i}\xi^{(m)}_{l,i} = \sigma^{(m)}\xi^{(m)}_{k,j}.$$

For the modes with non-zero eigenvalues, the forced equation (9*b*) would oscillate around a steady-state value (if the forcing term were constant in time). But modes with zero eigenvalue grow linearly in time (again for a constant forcing) which may lead to substantial vortex distortion and induce strong additional drift velocities of the vortex.

3.6. *Model limits*

We are dealing with intense vortices that can be described by the quasi-geostrophic equations, i.e. vortices for which $\epsilon = \beta L/\hat{\Omega} \ll 1$ and $R_o = U/fL = \hat{\Omega}/f \ll 1$. There is no contradiction implicit in these assumptions, rather the vortex rotation rate must satisfy $\beta L \ll \hat{\Omega} \ll f$, which is the case for many geophysical vortices.

When the flat bottom case is considered, there exists a barotropic mode with an associated Green function decreasing slowly for large r (A4) in Appendix A). It can also be proven (see Morel & McWilliams 1996) that, in that case, if the bulk integral of the potential vorticity anomaly is not zero initially, the vortex is not isolated and its associated velocity field decreases as $1/r$ in each layer. Our problem has then no solution because the integral in (7*d*) is not defined.

To avoid this degeneracy we can consider either a model with finite barotropic radius of deformation (Sutyrin 1988) or a model with an infinitely deep lower layer and set $\Upsilon = 1$ in (1*e*). This model filters out the barotropic mode and makes the solution tractable. If the barotropic mode is taken into account and is associated with an infinite radius of deformation, we must define isolated vortices with zero total potential vorticity anomaly. For the piecewise-constant potential vorticity structures considered here, this means that the potential vorticity jumps $\Delta_{k,j}$ and radii $r_{k,j}$ must satisfy $\Sigma_{k,j}\, H_k\, \Delta_{k,j} r^2_{k,j} = 0$.

4. Comparison between numerical solutions and theory

Let us now consider the case of a vortex with two contours, the first one in layer k_1 and associated with $r_{k_1,1} = r_1$, $\eta_{k_1,1} = \eta_1$, $\Delta_{k_1,1} = \Delta_1$, and the second one in layer k_2 and associated with $r_{k_2,1} = r_2$, $\eta_{k_2,1} = \eta_2$, $\Delta_{k_2,1} = \Delta_2$. Notice that the two contours can be in the same layer if $k_2 = k_1$. We have

$$\overline{\Omega}_k(r) = -\frac{1}{r}\sum_n P^{(n)}_k[\alpha^{(n)}_{k_1}\Delta_1 G^{(n)}_1(r|r_1) + \alpha^{(n)}_{k_2}\Delta_2 G^{(n)}_1(r|r_2)].$$

If we assume that the first contour in layer k_1 stays centred ($\eta_1 = 0$), (9*b*) gives the equation for the evolution of η_2:

$$\frac{\partial}{\partial t}\eta_2 - i\sigma^{(2)}\eta_2 = i\frac{\phi_{k_2}(r_2,t)}{r_2} - i\frac{\phi_{k_1}(r_1,t)}{r_1}$$
$$= \sum_{n,l}\alpha^{(n)}_l \int\left[\frac{P^{(n)}_{k_1}}{r_1}G^{(n)}_1(r_1|r) - \frac{P^{(n)}_{k_2}}{r_2}G^{(n)}_1(r_2|r)\right](\exp(i\overline{\Omega}_l(r)t) - 1)r\,dr \qquad (10a)$$

with

$$\sigma^{(2)} = -\frac{1}{r_2}\sum_n P_{k_2}^{(n)}\alpha_{k_1}^{(n)}\Delta_1 G_1^{(n)}(r_2|r_1) - \frac{1}{r_1}\sum_n P_{k_1}^{(n)}\alpha_{k_2}^{(n)}\Delta_2 G_1^{(n)}(r_1|r_2). \tag{10b}$$

equation (10*a*) is easily integrated and gives

$$\eta_2 = \sum_{n,l} -\mathrm{i}\alpha_l^{(n)}\int\left[\frac{P_{k_1}^{(n)}}{r_1}G_1^{(n)}(r_1|r) - \frac{P_{k_2}^{(n)}}{r_2}G_1^{(n)}(r_2|r)\right] \times\left[\frac{\exp(\mathrm{i}\overline{\Omega}_k(r)t) - \exp(\mathrm{i}\sigma^{(2)}t)}{\overline{\Omega}_k(r) - \sigma^{(2)}} + \frac{1-\exp(\mathrm{i}\sigma^{(2)}t)}{\sigma^{(2)}}\right] r\mathrm{d}r \tag{11}$$

The translation velocity of the vortex centre is given by (9*a*) and can be integrated with respect to time to give an analytical expression for the trajectory. We get

$$x + \mathrm{i}y = \frac{1}{r_1}\sum_{n,k} P_{k_1}^{(n)}\alpha_k^{(n)}\left(-\frac{r_1 t}{\gamma_n^2} + \int \mathrm{d}r r G_1^{(n)}(r_1|r)\frac{1-\exp(\mathrm{i}\overline{\Omega}_k(r)t)}{\mathrm{i}\overline{\Omega}_k(r)}\right) + \frac{\mathrm{i}}{r_1}\left[\sum_n P_{k_1}^{(n)}\alpha_{k_2}^{(n)}\Delta_2 G_1^{(n)}(r_1|r_2)\right]\int_0^t \eta_2 \mathrm{d}t. \tag{12}$$

The special case of a single contour is obtained if we set $\Delta_2 = 0$ in the previous equations, and in particular, only the first term of the right-hand side remains in (12). This term is associated with the advection of planetary vorticity and describes an acceleration up to the maximum long-wave speed, γ_n^{-2} for the nth mode. The additional drift associated with the second term results either from the horizontal distortion of the vortex core (if both contours are in the same layer) or from vertical tilting of the vortex core, which is a specific baroclinic effect. Notice that, as the bulk integral of the potential vorticity anomaly is usually not zero here, (12) is only defined when the barotropic mode has been filtered out. We have thus only considered the case of an infinitely deep lower layer. In each experiment, the first contour is located in the first layer ($k_1 = 1$), and we have chosen $r_1 = r_2 = 0.5$, $\Delta_1 = 1$, $\epsilon = 0.1$, $s_1 = 1$, $s_2 = 2$ and $h_1 = 0.25$.

As we are dealing with piecewise-constant potential vorticity, the centre of a contour is rather difficult to track in numerical simulations. Therefore, we have computed the trajectory of a streamfunction extrema. There is a slight difference between the trajectory of the extrema of the streamfunction and the centre of the contour, but it can be calculated analytically (see Appendix B), and we have thus chosen to make comparisons using trajectories of streamfunction extrema.

4.1. *Single contour case*

Vortex trajectories according to (12) and to the numerical model for the single contour case are shown in figure 2(*a*) for a reduced-gravity model (one layer with a passive lower layer) and in figure 2(*b–d*) for a two-and-a-half layer model (two active layers with a passive lower layer) and various thicknesses for the second layer h_2 (see table 1). In these plots, the trajectory obtained from the quasi-geostrophic numerical model (dashed line) and predicted by our analytical calculations (thin for the contour center and bold for the streamfunction extremum) are represented for a period of 100 non-dimensional time units together with the position of the vortex centre every 10 time units.

Equation (6*e*) shows that at small times, the dipolar component of potential vorticity is oriented meridionally, with a positive anomaly to the west and a negative one to the east (we have considered only cyclones in our experiments). Figure 2 shows

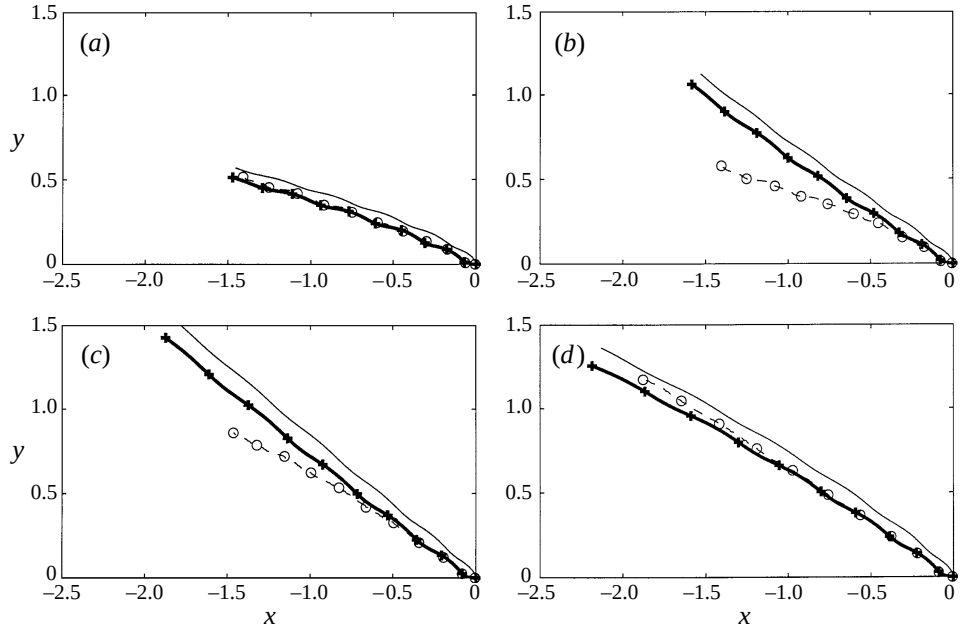

FIGURE 2. Comparisons between numerical solutions (dashed) and theoretical trajectories (bold for the streamfunction extrema and thin for the contour centre) for (*a*) one contour in a reduced-gravity model and, (*b–d*) one contour in a two-and-a-half layer model with different background stratification given in table 1: (*b*) experiment 1, $h_2 = 10$, (*c*) experiment 2, $h_2 = 2$, (*d*) experiment 3, $h_2 = 0.5$.

Experiment no.	h_2	$1/\gamma^{(1)}$	$1/\gamma^{(2)}$
Reduced gravity	∞	0.5	∞
1	10	0.49	2.26
2	2	0.46	1.08
3	0.5	0.35	0.71

TABLE 1. Experiments with one contour: stratification characteristics

that for the dipolar component of the streamfunction, this structure yields a positive anomaly to the east and a negative one to the west, corresponding to an initial westward displacement of the streamfunction minimum. As this dipolar component is also associated with a northward current at the contour centre, the streamfunction minimum starts to drift northward. The weak wavy patterns that can be seen in both the numerical and analytical trajectories are more pronounced in the propagation speed (see SF94). These are due to the revolution of particles around the vortex centre at a rotation rate $\overline{\Omega}$ and are associated with the oscillatory nature of the integrals in (12).

The period of time for which the theoretical results should be accurate is $T \ll (\epsilon r_0)^{-1} = 20$. In fact, the plots show that the theoretical predictions are very close to the numerical solutions (the deviation does not exceed 20% of the vortex radius) at least up to 40 time units. Some strong discrepancies then appear when the depth of the second layer h_2 is large, that is to say when the rotation rate Ω_2 is weak (as there is no potential vorticity anomaly in the second layer, the rotation rate is weaker for a larger layer depth). This is due to dispersion by Rossby waves in this layer. Indeed, the

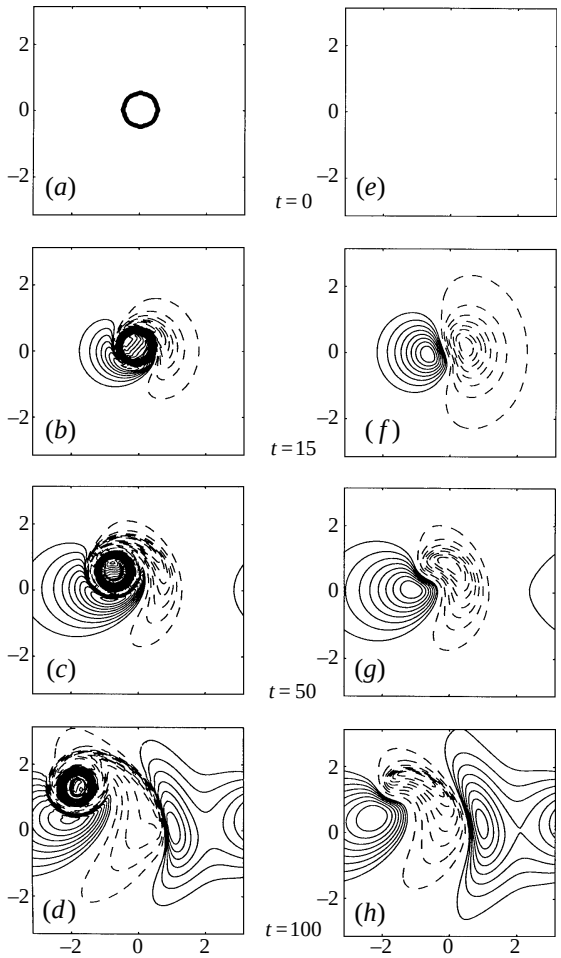

FIGURE 3. Evolution of the potential vorticity anomaly in layer 1 (*a–d*) and 2 (*e–h*) for experiment 3 (single contour case in the first layer and 2.5 model with $h_2 = 0.5$), and at $t = 0$, 15, 50 and 100 time units. Negative values are dashed. Notice the development of the beta-gyre and its initial dipolar form at $t = 15$.

maintenance of the vortex identity, which is a hypothesis of our theoretical model, is ensured by the nonlinear term in (2*a*) (see McWilliams & Flierl 1989). If the rotation rate is weak, ϵ is no longer a small parameter and the linearization of the equations is not valid. In that case, the vortex will undergo dispersion by Rossby waves whose effect will be to dissipate the motion in the second layer. Thus, in the case of large h_2 the vortex trajectory is well predicted by the reduced-gravity model (where no motion is assumed in the second layer) (cf. figure 2*a,b*). When the rotation rate is strong in both layers of the model, the theoretical and numerical plots show very good agreement (the deviation does not exceed 20% of the vortex radius) up to more than 70 time units for the reduced-gravity case (figure 2*a*) and for $h_2 = 0.5$ (figure 2*d*). The correction due to the different definitions of the 'center' of the vortex (streamfunction extrema or centre of a contour) is rather small and can be neglected in practice; it is shown here to illustrate the agreement between numerical and analytical models.

Figure 3 shows the evolution of the potential vorticity anomaly in both active layers for $h_2 = 0.5$. The dipolar structure of the beta-gyres is clear, especially at the

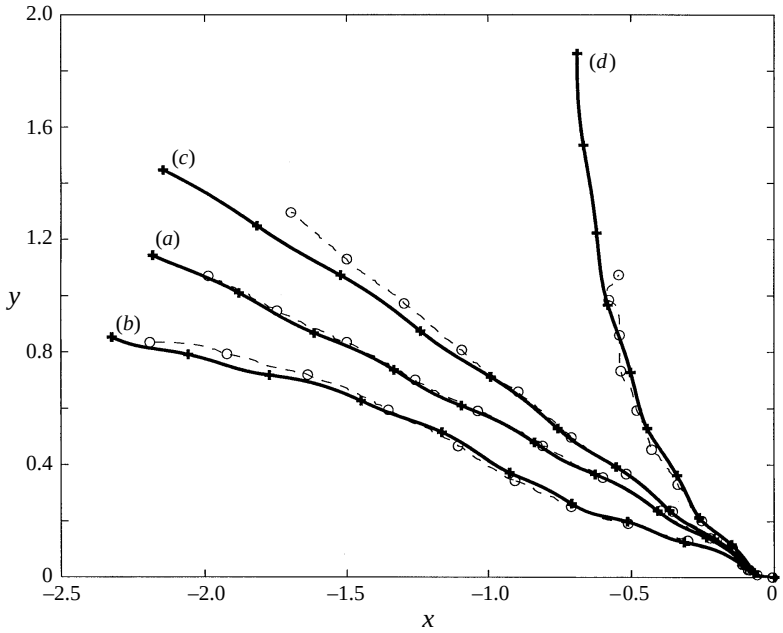

FIGURE 4. Comparisons between numerical solutions (dashed) and theoretical trajectories (solid) for two contours in a two-and-a-half layer model. The stratification is kept the same in all experiments, however the potential vorticity changes in the second layer. (*a*) Experiment 1, $\Delta_2 = 0.1$, (*b*) experiment 2, $\Delta_2 = 1$, (*c*) experiment 3, $\Delta_2 = -0.1$, (*d*) experiment 4, $\Delta_2 = -0.5$.

beginning of the simulation. At later stages, however, its shape becomes disturbed by higher asymmetric modes which were neglected at leading order. Notice that the orientation of the dipole axes is different in each layer, which leads to different displacement direction and amplitude in comparison with the one-layer case.

4.2. *Two-contour case*

Here, comparisons are made to test the theoretical prediction for the effect of the vertical tilting on the vortex trajectory. Thus, experiments were done with a two-and-a-half layer model with $k_2 = 2$, $h_2 = 0.5$ and various Δ_2. Again, the trajectories were calculated for 100 non-dimensional time units. The corresponding trajectories (dashed for numerical solutions and solid for the analytical ones) are given in figure 4. The development of the vertical tilting is represented by the horizontal separation between the contour centres in different layers: $(X2 - X1, Y2 - Y1)$, where (Xi, Yi) is the contour centre of the ith layer. It is shown in figure 5 for experiments 2 and 4 ($\Delta_2 = 1$ and $\Delta_2 = -0.5$, respectively).

When $\Delta_2 > 0$, the agreement is, as for the single contour case with a strong rotation in the second layer, very good for up to 70–80 time units (the deviation does not exceed 20% of the vortex radius), so that the analytical model gives accurate information on the trajectory up to at least 100 time units. The vortex tilting (figure 5*a*) is well reproduced for the same period and remains small. Thus the effect of the vertical tilting is, in this case, moderate and the propagation is still dominated by advection of planetary vorticity. Note also that when the vortex becomes stronger (that is to say when Δ_2 increases), the meridional displacement is weaker (see figure 4*a,b*). In fact, as can be expected from (12), for a stronger vortex with higher rotation rate,

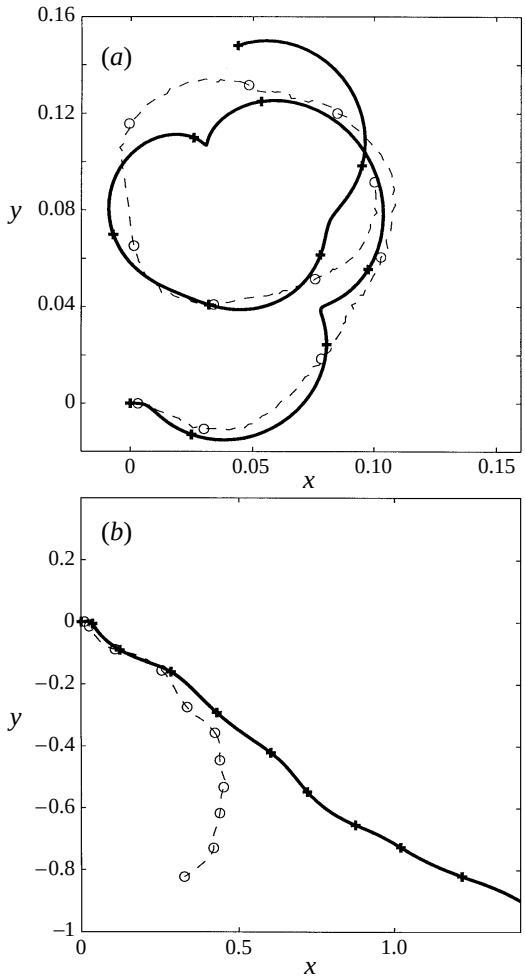

FIGURE 5. Comparison between numerical solutions (dashed) and theoretical prediction (solid) for the separation between the two contour centres $(X_2 - X_1, Y_2 - Y_1)$: (*a*) experiment 2, $\Delta_2 = 1$, (*b*) experiment 4, $\Delta_2 = -0.5$.

the period of acceleration toward the maximum long-wave speed is shorter and the vortex reaches the state when the propagation is predominantly westward sooner.

When $\Delta_2 < 0$, the vortex structure is apparently unstable and undergoes a strong deformation. Indeed, figure 5(*b*) shows that the vertical tilting between contours in two layers grows to values comparable with a vortex diameter. Thus, the influence of the self-advection due to tilting of the vortex core drastically modifies the vortex propagation. This was demonstrated also by Morel & McWilliams (1996). However, the initial prediction is quite close to the numerical solution up to 40–50 time units (again, the deviation of the vortex centre does not exceed 0.1), and the direction of propagation is well described by the analytic theory.

Figure 6 shows the evolution of the potential vorticity patches of each layer on the same graph (solid contour for the first layer, dashed for the second) for experiments 2 and 4. It shows that, in addition to the large tilting of the vortex core when $\Delta_2 = -0.5$, the vortex undegoes a strong mode-two deformation and become elliptical, whereas for $\Delta_2 = 1$, the vortex structure preserves its axisymmetry.

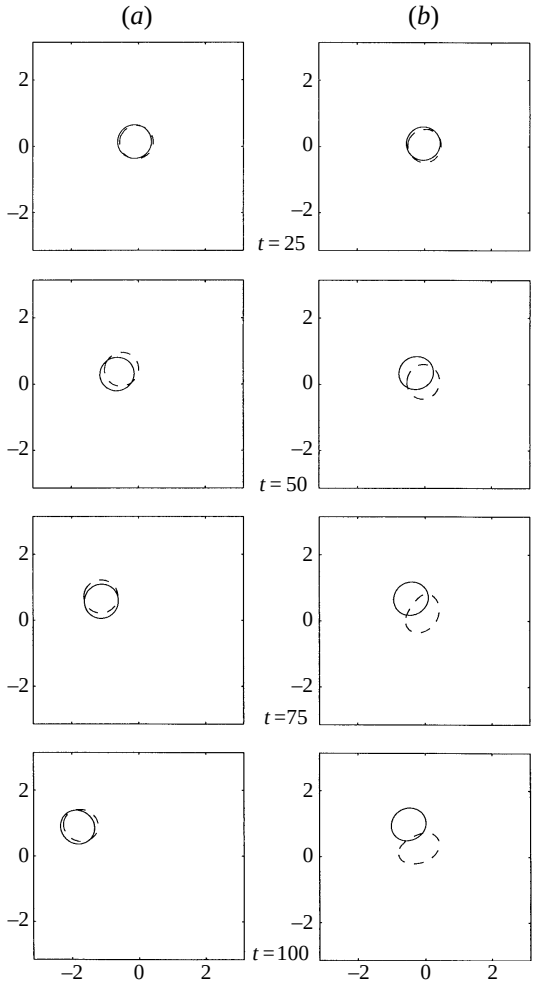

FIGURE 6. Evolution of the potential vorticity contours in both layers every 25 time units for (*a*) experiment 2, $\Delta_2 = 1$, and (*b*) 4, $\Delta_2 = -0.5$ (two contours and a two-and-a-half layer model). The dashed contour is associated with the second layer and the solid one with the first layer.

5. Summary and discussion

We have presented an analytical model for the prediction of vortex trajectories on the β-plane in a multi-layer model. In addition to the generation of the potential vorticity anomaly by planetary vorticity advection and horizontal deformations of the vortex core, we have found that, when stratification is taken into account, the vertical tilting of the vortex core can drastically modify the propagation too.

This model yields an explicit relationship between the background stratification, the vortex structure and its motion. Thus, it can shed light on some numerical results such as the strong dependency of a vortex trajectory on its vertical structure (Morel & McWilliams 1996). Note also that the present model can be easily generalized to include bottom topography or a vertically sheared mean current. In particular, Hogg & Stommel (1990) have described a mechanism for the advection of subsurface vortices by an upper layer current, but they neglected the effect of the interface displacement associated with the vertical shear of the current. Morel (1995) showed

that the dynamics of some vortices were in fact very sensitive to this interface deviation and that their displacement could be very different from that predicted by Hogg & Stommel. The analytical theory developed is able to take into account this effect.

As mentioned previously, this analytical model is based on an expansion and is *a priori* valid only for times smaller than the Rossby wave period ($T \ll 1/\epsilon r_0$). It turns out, however, that in most of our numerical experiments, when the assumption of strong rotation is valid in each layer, the analytical prediction is very accurate up to several Rossby wave periods and gives useful insight into the vortex behaviour. Although we did not compute the next-order terms, which is necessary to check the validity of our analytical model at the slow timescale ϵt, the leading-order solution apparently gives a good representation for times of the order of the characteristic Rossby wave timescale. This indicates that the neglected nonlinear terms act to maintain the asymmetric part of the flow field small.

We have presented eight comparisons between this analytic model and a numerical quasi-geostrophic one. We have performed several other experiments with up to two contours and three layers and with different initial conditions, both for the vortex structure and background stratification. These experiments led to the same conclusion: the theoretical formulae can be considered accurate up to 2–5 Rossby wave periods. The strongest discrepancies between the theoretical prediction and numerical results occur either when the initial vortex structure is not stable and the relative displacement of the contours becomes large, or when the rotation rate is weak in one layer and the vortex flow undergoes dispersion.

Finally, these comparisons between numerical and analytical models also show that the numerical pseudospectral model can cope with piecewise-constant potential vorticity structure, and is reliable for the period of time considered here.

Part of this work was done at Institut de Mécanique de Grenoble, during G. G. Sutyrin's visit and while Y. G. Morel was a PhD student at the Laboratoire des Ecoulements Géophysiques et Industriel de Grenoble (LEGI). We would like to especially thank Dr William Dewar for his help and advice. We are also grateful to Drs Xavier Carton, Jacques Verron and Christian Le Provost for stimulating discussions and comments and we would also like to thank all the people that contributed to the friendly atmosphere at LEGI. This study was made possible by a grant of the Service Hydrographique et Océanographique de la Marine (SHOM) and is a contribution to the SHOM/CMO research program "Processus Associés aux Modèles Intermédiaires et Régionaux".

Appendix A. Vertical modes

For perturbations having an azimuthal mode one, equations (5), (6*a*) and (6*d*) can all be written in the same way for the radial variation of each quantity and take the form

$$\nabla_1^2 \varphi_k + \frac{s_{k-1}}{h_k}(\varphi_{k-1} - \varphi_k) + \frac{s_k}{h_k}(\varphi_{k+1} - \varphi_k) = \Gamma_k \tag{A1}$$

with

$$\nabla_1^2 = \frac{1}{r}\frac{\partial}{\partial r} r \frac{\partial}{\partial r} - \frac{1}{r^2}.$$

This equation can be solved in terms of vertical modes $\boldsymbol{P}^{(n)} = (P_1^{(n)}, ..., P_k^{(n)}, ..., P_N^{(n)})$ associated with the vortex-stretching matrix in (2*b*), so that

$$\frac{s_{k-1}}{h_k}(P_{k-1}^{(n)} - P_k^{(n)}) + \frac{s_k}{h_k}(P_{k+1}^{(n)} - P_k^{(n)}) = -\gamma_n^2 P_k^{(n)}$$

where $\gamma_n^{-1} = R_n/\hat{R}$ is the non-dimensional radius of deformation of the nth mode. We also define a matrix $\boldsymbol{\alpha}$, with coefficients $\alpha_k^{(n)}$, by orthogonality conditions with vertical modes ($\sum_n \alpha_k^{(n)} P_l^{(n)} = \delta_{kl}$). $\boldsymbol{\alpha}$ is the inverse of the matrix $\boldsymbol{P}$ whose column are the eigenvectors $\boldsymbol{P}^{(n)}$ (so that we also have $\sum_k \alpha_k^{(m)} P_k^{(n)} = \delta_{mn}$). Thus, if we set

$$\varphi_k = \sum_n \varphi^{(n)} P_k^{(n)}, \quad \Gamma_k = \sum_n P_k^{(n)} \Gamma^{(n)}, \quad \Gamma^{(n)} = \sum_l \alpha_l^{(n)} \Gamma_l,$$

$\varphi^{(n)}$ satisfies

$$\nabla_1^2 \varphi^{(n)} - \gamma_n^2 \varphi^{(n)} = \Gamma^{(n)}. \tag{A2}$$

A Green function $G_1^{(n)}(r|r')$ for the Helmholtz's operator of the left-hand side (when $\Gamma^{(n)} = \delta(r' - r)$) is given by (see Abramowitz & Stegun 1970)

$$G_1^{(n)}(r|r') = \begin{cases} -r' I_1(\gamma_n r) K_1(\gamma_n r'), & r < r' \\ -r' I_1(\gamma_n r') K_1(\gamma_n r), & r > r', \end{cases} \tag{A3}$$

with I_1 and K_1 being modified Bessel functions. Note, that in the rigid-lid approximation, and for the flat bottom case, there exist a barotropic mode associated with $\gamma_0 = 0$, so that (A3) becomes

$$G_1^{(0)}(r|r') = \begin{cases} -r/2, & r < r' \\ -r'^2/2r, & r > r'. \end{cases} \tag{A4}$$

The solution of (A2) is thus

$$\varphi^{(n)}(r) = G_1^{(n)}(r|r')$$

if $\Gamma^{(n)}(r) = \delta(r - r')$ and

$$\varphi^{(n)}(r) = \int G_1^{(n)}(r|r') \Gamma^{(n)}(r') \mathrm{d}r'$$

otherwise. So the solution of (A1) is given by

$$\varphi_k(r) = \sum_{n,l} P_k^{(n)} \alpha_l^{(n)} \int G_1^{(n)}(r|r') \Gamma_l(r') \mathrm{d}r' \tag{A5}$$

Appendix B. Trajectory correction

In numerical simulations we calculate the trajectory of a streamfunction extrema $(x_0^\psi(t), y_0^\psi(t))$. Its displacement relative the vortex centre defined by (9*a*,*b*) can be calculated from the condition $\nabla\psi = 0$. We get

$$x_0^\psi - x_0 = -\frac{1}{\overline{\Omega}_L(0)} \left(\frac{\partial(\phi_L + \Phi'_L)}{\partial x} \right)_{r=0}, \qquad y_0^\psi - y_0 = -\frac{1}{\overline{\Omega}_L(0)} \left(\frac{\partial(\phi_L + \Phi'_L)}{\partial y} \right)_{r=0} \tag{B1}$$

which after a few calculations gives

$$x_0^{\psi} - x_0 + \mathrm{i}(y_0^{\psi} - y_0) = \frac{1}{\overline{\Omega}_{k_0}(0)} \left[\sum_{n,l} -\mathrm{i} P_{k_0}^{(n)} \alpha_l^{(n)} Z_k^{(n)} + \sum_{n,l,m} P_{k_0}^{(n)} \alpha_l^{(n)} \Delta_{l,m} r_{l,m} K_1(\gamma_n r_{l,m}) \tfrac{1}{2} \gamma_n \eta_{l,m} \right] \tag{B2}$$

where

$$Z_k^{(n)} = \lim_{r \to 0} \frac{F_k^{(n)}(r,t)}{r} = -\frac{\gamma_n}{2} \int_0^{\infty} K_1(\gamma_n r)(\mathrm{e}^{\mathrm{i}\overline{\Omega}_k t} - 1) r^2 \mathrm{d}r \tag{B3}$$

REFERENCES

Abramowitz, M. & Stegun, I. A. (Eds.) 1970 *Handbook of Mathematical Functions.* National Bureau of Standards, pp. 231–233.

Chassignet, E. P. & Cushman-Roisin, B. 1991 On the influence of a lower-layer on the propagation of nonlinear oceanic eddies. *J. Phys. Oceanogr.* **21**, 939–957.

Fiorino, M. & Elsberry, R. L. 1989 Some aspects of vortex structure related to tropical cyclone motion. *J. Atmos. Sci.* **46**, 975–990.

Flatau, M., Schubert W. H. & Stevens, D. E. 1994 The role of baroclinic processes in tropical cyclone motion: The influence of vertical tilt. *J. Atmos. Sci.* **51**, 2589–2601.

Hogg, N. & Stommel, H. 1990 How currents in the upper thermocline could advect meddies deeper down. *Deep-Sea Res.* **37**, 613–623.

Kamenkovich, V. M., Koshlyakov, M. N. & Monin, A. S. 1986 *Synoptic Eddies in the Ocean.* Reidel.

Khain, A. P. & Sutyrin, G. G. 1983 *Tropical Cyclones and their Interaction with the Ocean.* Gidrometeoizdat, Leningrad (in Russian).

McWilliams, J. C. 1985 Submesoscale, coherent vortices in the ocean. *Rev. Geophys.* **23**, 165–182.

McWilliams, J. C. & Flierl, G. R. 1979 On the evolution of isolated, nonlinear vortices. *J. Phys. Oceanogr.* **9**, 1155–1182.

Morel, Y. 1995 The influence of an upper thermocline current on intrathermocline eddies. *J. Phys. Oceanogr.* **25**, 3247–3252.

Morel, Y. & McWilliams, J. C. 1997 Evolution of isolated interior vortices in the ocean. *J. Phys. Oceanogr.* in press.

Orszag, S. 1971 Numerical simulation of incompressible flows within simple boundaries. I. Galerkin (spectral) representations. *Stud. Appl. Maths* **50**, 293–328.

Pedlosky, J. 1987 *Geophysical Fluid Dynamics.* Springer.

Peng, M. S. & Williams, R. T. 1990 Dynamics of vortex asymmetries and their influence on vortex motion on a β–plane. *J. Atmos. Sci.* **47**, 1987–2003.

Polvani, L. M., Zabusky, N. J. & Flierl, G. R. 1989 Two-layer geostrophic vortex dynamics. Part 1. Upper-layer V-states and merger. *J. Fluid Mech.* **205**, 215–242.

Reznik, G. M. & Dewar, W. K. 1994 An analytic theory of distributed axisymmetric barotropic vortices on the β-plane. *J. Fluid Mech.* **269**, 301–321.

Shapiro, L. J. 1992 Hurricane vortex motion and evolution in a three-layer model. *J. Atmos. Sci.* **49**, 140–153.

Smith, R. K. & Ulrich, W. 1990 An analytical theory of tropical cyclone motion using a barotropic model. *J. Atmos. Sci.* **47**, 1973–1986.

Smith, R. K., Ulrich, W. & Dietachmayer, G. 1990 A numerical study of tropical cyclone motion using a barotropic model. Part I: The role of vortex asymmetries. *Q. J. R. Met. Soc.* **116**, 337–362.

Sutyrin, G. G. 1987 The beta–effect and the evolution of a localized vortex. *Sov. Phys. Dokl.* **32**(10), 791–793.

Sutyrin, G. G. 1988 Motion of an intense vortex on a rotating globe. *Fluid Dyn.* **23**(4), 215–223.

Sutyrin, G. G. 1989 Forecast of intense vortex motion with an azimuthal modes model. In *Mesoscale/Synoptic Coherent Structures in Geophysical Turbulence* (ed. J. C. J. Nihoul & B. M. Jamart), pp. 771–782.

Sutyrin, G. G. & Flierl, G. R. 1994 Intense vortex motion on the beta–plane: Development of the beta gyres. *J. Atmos. Sci* **51**, 773–790 (referred to herein as SF94).

Sutyrin, G. G., Hesthaven, J. S., Lynov, J. P. & Rasmussen, J. J. 1994 Dynamical properties of vortical structures on the beta-plane. *J. Fluid Mech.* **268**, 103–131.